Author(s): Izotov, I.; Kalvas, Taneli; Koivisto, Hannu; Kronholm, Risto; Mansfeld, D.; Skalyga, V.; Tarvainen, Olli

Title: Broadband microwave emission spectrum associated with kinetic instabilities in minimum-B ECR plasmas

Year: 2017

Version:

Please cite the original version:

Izotov, I., Kalvas, T., Koivisto, H., Kronholm, R., Mansfeld, D., Skalyga, V., & Tarvainen, O. (2017). Broadband microwave emission spectrum associated with kinetic instabilities in minimum-B ECR plasmas. Physics of Plasmas, 24(4), Article 043515. https://doi.org/10.1063/1.4981387

Broadband microwave emission spectrum associated with kinetic instabilities in minimum-B ECR plasmas

I. Izotov, T. Kalvas, H. Koivisto, R. Kronholm, D. Mansfeld, V. Skalyga, and O. Tarvainen

Citation: Physics of Plasmas **24**, 043515 (2017); doi: 10.1063/1.4981387
View online: http://dx.doi.org/10.1063/1.4981387
View Table of Contents: http://aip.scitation.org/toc/php/24/4
Published by the American Institute of Physics

Broadband microwave emission spectrum associated with kinetic instabilities in minimum-B ECR plasmas

I. Izotov,[1] T. Kalvas,[2] H. Koivisto,[2] R. Kronholm,[2] D. Mansfeld,[1] V. Skalyga,[1] and O. Tarvainen[2]
[1]*Institute of Applied Physics, Russian Academy of Sciences (IAP RAS), 603950, 46 Ulyanova st., Nizhny Novgorod, Russia*
[2]*Department of Physics, University of Jyvaskyla, PO Box 35 (YFL), 40500 Jyvaskyla, Finland*

(Received 22 December 2016; accepted 5 April 2017; published online 20 April 2017)

Plasmas of electron cyclotron resonance ion sources (ECRISs) are prone to kinetic instabilities due to the resonant heating mechanism resulting in anisotropic electron velocity distribution. Frequently observed periodic oscillations of extracted ion beam current in the case of high plasma heating power and/or strong magnetic field have been proven to be caused by cyclotron-type instabilities leading to a notable reduction and temporal variation of highly charged ion production. Thus, investigations of such instabilities and techniques for their suppression have become important topics in ECRIS research. The microwave emission caused by the instabilities contains information on the electron energy distribution and growth mechanism of the instability. The emission has been studied earlier in the frequency range of 8–14 GHz allowing us to deduce the probable excited mode. A more detailed study of the microwave emission spectrum of a minimum-B ECR plasma, sustained by 14 GHz microwave radiation, is presented in this work. It was found that the frequencies of the microwaves emitted by the plasma consist of several harmonics of the main band and extend from 6 GHz up to 25 GHz, being independent of the plasma parameters. *Published by AIP Publishing*. [http://dx.doi.org/10.1063/1.4981387]

INTRODUCTION

Conventional Electron Cyclotron Resonance Ion Sources (ECRISs) with a minimum-B magnetic field configuration have been widely used for injection of multicharged ion beams into accelerators for over 40 years. The physical principles of these devices are rather well-studied although there are still numerous unexplained experimental observations related to their plasmas. A long-standing inexplicable observation has been the ms-scale oscillation of the extracted ion beam current.[1–3] Such oscillations are especially problematic for applications of high performance ECR ion sources requiring supreme temporal stability, e.g., hadron therapy[4] and material modification.[5]

The magnetic field of modern ECRISs (see, e.g., Refs. 6 and 7) is a superposition of solenoid and sextupole fields. The resulting minimum-B topology provides a closed ECR surface for efficient resonant energy transfer from microwaves to the plasma electrons, enables sufficient plasma confinement for the step-wise ionization of high charge states, and suppresses magneto-hydrodynamic instabilities.[8] The electron energy distribution resulting from the resonant heating and long confinement time of energetic electrons[9] is strongly anisotropic and is considered to consist of (at least) two main populations: cold (and warm) electrons with an average energy of $E_{e,cold} = 10\,eV–10\,keV$ and hot electrons with $E_{e,hot} > 10\,keV$ up to 1 MeV.[10,11] Such non-equilibrium plasmas are prone to kinetic instabilities driven by warm and hot electrons whose transverse (with respect to the external magnetic field) velocity $V_\perp$ dominates over the longitudinal velocity $V_\parallel$.[12,13]

It has been proven that the kinetic instabilities of cyclotron type are the reason for the aforementioned periodic oscillation of the extracted beam current with a maximum amplitude of several tens of percent[14,15] and simultaneous powerful bursts of microwave and x-ray radiation. It has been shown that the cyclotron instabilities lead to significant electron losses and subsequent increase of the plasma potential perturbing the ion confinement[16] at temporal interval which is less than the production time[17] of high charge state ions. Therefore, the kinetic instabilities are especially detrimental for high charge state production as demonstrated in Refs. 15 and 16. Since the microwave power is one of the main parameters determining the threshold for the instabilities,[14] it implies that further increase of heating power, being probably the most common brute force method of improving ECRIS performance, will not be successful without suppressing the instabilities.

Cyclotron instabilities arise from the anisotropy of electron distribution in the velocity space. A characteristic feature of the cyclotron instability is the emission of electromagnetic (EM) radiation due to resonant amplification of plasma waves by "hot" electrons. The microwave emission during the onset of the cyclotron instability has been observed in various experiments studying ECR-heated plasmas in a simple mirror (see, e.g., Refs. 18 and 19) and minimum-B traps (see, e.g., Refs. 20 and 21).

This work is an extension of studies reported in Ref. 22, where the microwave emission of the CW plasma sustained by 14 GHz microwave radiation was studied in the range of 8–15 GHz. The experimental setup has been recently improved and equipped with a 33 GHz bandwidth oscilloscope, which has enabled the detection of the microwave signal in the range of 7.9 up to 25 GHz. Under certain

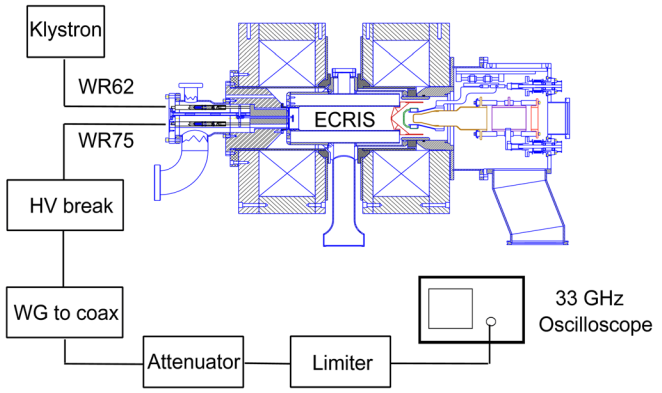

FIG. 1. Schematic drawing of the experimental setup.

conditions, the frequency range can be broadened to 0–25 GHz as explained in the Experimental Results and Discussion Section. The extended bandwidth has allowed investigating the whole range of emission frequencies within the complete range of electron gyrofrequencies corresponding to closed magnetic field isosurfaces (0.35–0.9 T for JYFL 14 GHz ECRIS) found in the minimum-B trap. Knowledge on the lower limit of the emitted frequencies enables estimating the energy of the electrons driving the instability.

EXPERIMENTAL SETUP

The experimental data were taken with the room-temperature A-ECR-U type JYFL 14 GHz ECRIS[23] operated with a single frequency (14.056 GHz) sustaining the plasma in the continuous (CW) mode. In the experiments described here, a klystron amplifier providing the microwave signal was connected to a WR-62 waveguide port of the ion source. The magnetic field of the ion source is generated by two solenoid coils and a permanent magnet sextupole resulting in a so-called minimum-B field configuration. The resonance condition for (cold) electron heating is satisfied on a closed (nearly) ellipsoidal surface with a constant magnetic field of $B_{ECR} = 0.5$ T. The magnetic field strength can be adjusted by varying the solenoid coil currents, which affects the injection and extraction mirror ratios as well as the B_{min}/B_{ECR}-ratio. The strength of the sextupole field on the plasma chamber wall at the magnetic pole is 1.07 T when the solenoids are not energized.[24] A complete description of the magnetic field profile can be found from Ref. 15. Frequencies emitted by the plasma were measured through a WR-75 waveguide port incorporated into the injection iron plug. The emitted microwave signal was guided into a Keysight DSOV334A Infiniium V-Series oscilloscope through WR-75 waveguide, vacuum window, high voltage break, waveguide-to-coaxial transition, power limiter, and tunable attenuator. The features of the oscilloscope—80 Gs/s sampling rate and 33 GHz bandwidth allowed direct recording of the waveforms of microwave pulses emitted by the plasma with a temporal resolution of 12.5 ps. It is emphasized that the coupling frequency-dependent efficiency between the plasma and the receiver (oscilloscope) is unknown. Hence, the measured emission spectra cannot be used to deduce the relative intensity of the emission throughout the probed frequency range but they rather indicate the frequency bands in which the microwave emission due to cyclotron-type instabilities occurs. A schematic figure of the ECRIS and the experimental setup is shown in Figure 1. The ion source was operated above the instability threshold levels,[14] i.e., $B_{min}/B_{ECR} > 0.75$ and > 400 W of 14 GHz microwave power, the magnetic field being the dominant factor defining the transition from the stable regime to the unstable regime.[14] The results obtained with oxygen in the pressure range of 4–5 $\times 10^{-7}$ mbar, being typical operating pressure for high charge state production, are reported hereafter. The pressure readings were measured outside the plasma chamber with an ionization gauge connected to a radial diagnostics port of the ion source.

EXPERIMENTAL RESULTS AND DISCUSSION

The microwave signal fed directly to the input channel of the oscilloscope through the attenuator and limiter was used to trigger the high sampling rate data acquisition of the microwave signal waveform. Figure 2 presents a typical waveform of the microwave signal recorded during a single instability event. The duration of the microwave emission in the given example is approximately 2 μs. The data were taken with

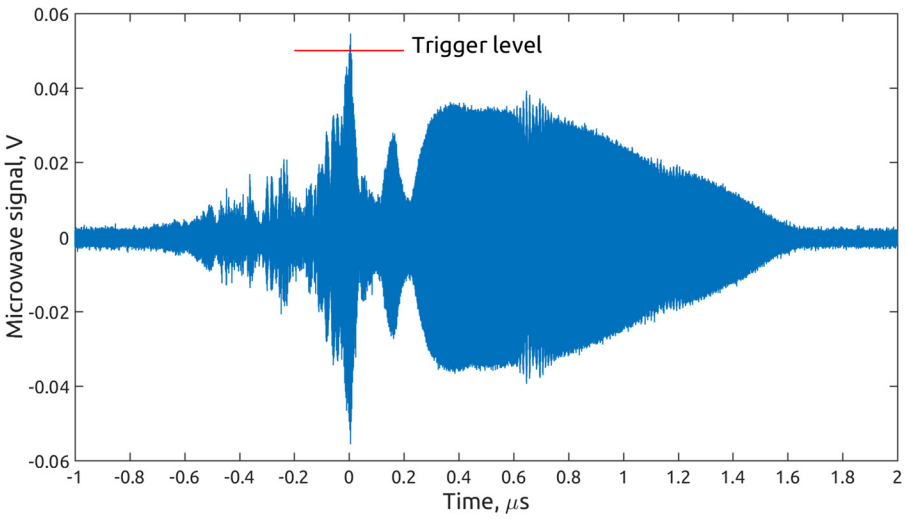

FIG. 2. An example of the microwave signal waveform. Oxygen plasma, 4.7 $\times 10^{-7}$ mbar, $B_{min}/B_{ECR} = 0.83$, 400 W microwave power.

oxygen plasma, at 4.7×10^{-7} mbar, $B_{min}/B_{ECR} = 0.83$ and 400 W of injected microwave power. Similar to previous experiments,[22] the emitted microwave signal was observed to consist of discrete packets lasting typically 100–1500 ns and separated by some hundreds of ns. Their relative magnitudes and temporal separations were observed to depend on the ion source settings, i.e., magnetic field strength and microwave power.

Figure 3 shows dynamic spectrograms of the typical microwave signal recorded at different magnetic field strengths, microwave powers, and oxygen pressures. The signals presented hereafter were treated with Goertzel algorithm to build the spectral power density, indicated with false color, in each time domain (~2 ns with 98% neighbour overlapping) in the range of 8–26 GHz with 20 MHz step. The data were taken with oxygen plasma, at 4.2×10^{-7} mbar, 600 W of klystron power, $B_{min}/B_{ECR} = 0.79$ (a) and $B_{min}/B_{ECR} = 0.83$ (b), and at 4.6×10^{-7} mbar, 300 W of klystron power, $B_{min}/B_{ECR} = 0.83$ (c) and $B_{min}/B_{ECR} = 0.87$ (d). These examples are presented to highlight that the microwave emission spectra exhibit certain common features, e.g., discrete emission bands, independent of the ion source settings. Furthermore, the spectrograms reveal a complex temporal structure of the signal. In particular, the emission spectra indicate the presence of a main emission band at 8.2–12.6 GHz and its second harmonic at 16.5–25.5 GHz, which has not been detected previously due to limited frequency range (formerly 8–15 GHz (Ref. 22)) of the experimental setup (harmonics of higher order cannot be excluded as well). The emission frequencies of the first and second harmonics decrease monotonically within a single instability event, which is a fundamental behaviour of all recorded data. The horizontal line at 14.056 GHz corresponds to the CW signal of the klystron coupled into the waveguide (with a subharmonic barely seen at 9.39 GHz). Although the coupling efficiencies of various frequencies into the diagnostic port are unknown, as well as the total power reflected from the plasma, it is worth noting that the measured spectral power density of the klystron signal is at least two orders of magnitude lower than the peak power of the instability signals. The horizontal line at 20.00 GHz is a digital artifact related to the sampling rate of the oscilloscope and subsequent analysis of the data.

Figure 4 shows two-dimensional frequency spectra of the signals shown in Fig. 3. The spectra are built in the following way: the signal is first divided into short time domains of 2 ns, the FFT of the signal is subsequently built inside each time domain, and finally all of the FFT results are summarized in a single plot. Such a way of plotting the 2D spectra allows us to emphasize the frequencies of short bursts unlike the regular FFT of the whole signal, which may suppress the signal of the emission bursts much shorter than the total record length.

Increasing the magnetic field strength leads to an increase in the number of wave packets and results in a broader range of emission frequencies. However, the central frequency of the first and subsequent packets is unaffected by the field strength. The spectra shown in Fig. 4 confirm the earlier[22] discovery of the dominant emission frequencies (in the range of 8–15 GHz) being independent of source parameters such as microwave power, magnetic field, and the gas pressure, in a wider range of frequencies.

In order to study whether microwave emission occurs at frequencies below the 7.9 GHz cut-off frequency of the waveguide, the waveguide connection between the ion source plasma chamber and the oscilloscope was replaced with a broadband short dipole antenna directed towards the ion source. The radiation diagram of the dipole antenna was

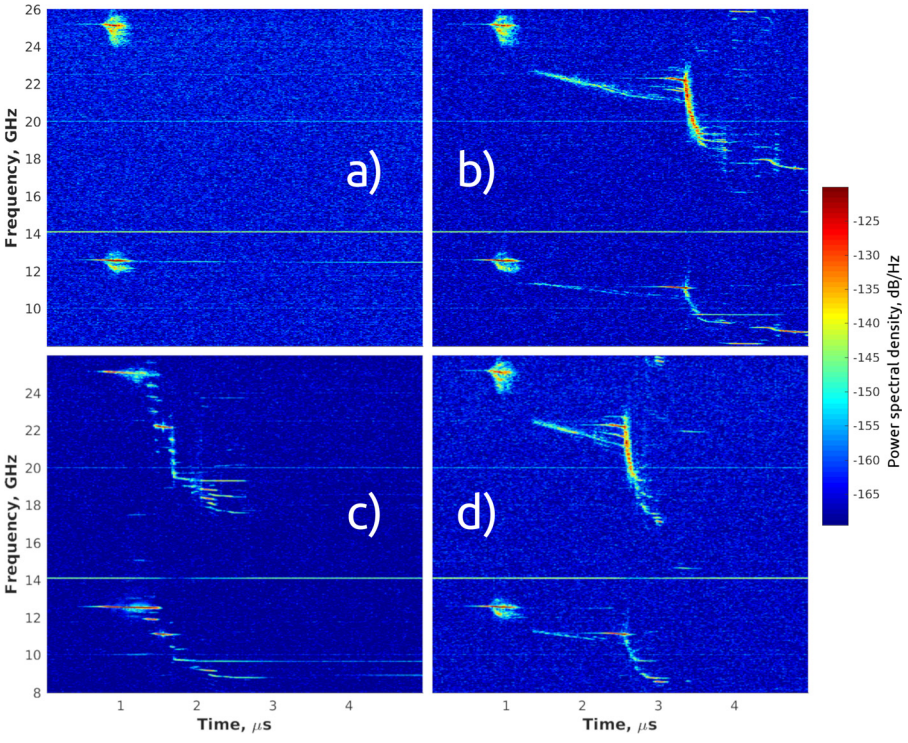

FIG. 3. Dynamic spectrograms of the emitted microwave signal. Oxygen plasma, at 4.2×10^{-7} mbar, 600 W of klystron power, $B_{min}/B_{ECR} = 0.79$ (a) and $B_{min}/B_{ECR} = 0.83$ (b); at 4.6×10^{-7} mbar, 300 W of klystron power, $B_{min}/B_{ECR} = 0.83$ (c) and $B_{min}/B_{ECR} = 0.87$ (d).

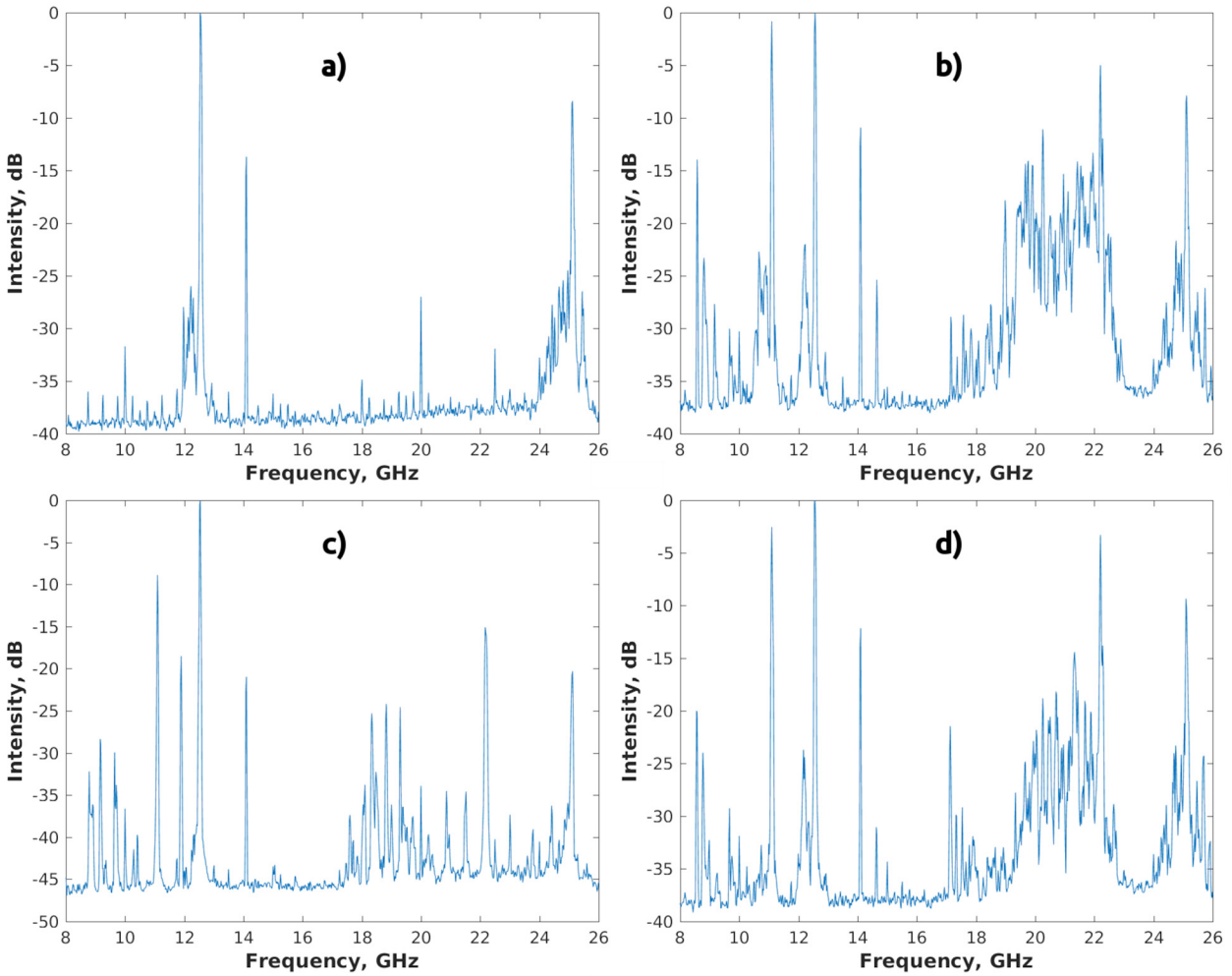

FIG. 4. 2-D spectra of signals. Oxygen plasma, at 4.2×10^{-7} mbar, 600 W of klystron power, $B_{min}/B_{ECR} = 0.79$ (a) and $B_{min}/B_{ECR} = 0.83$ (b); at 4.6×10^{-7} mbar, 300 W of klystron power, $B_{min}/B_{ECR} = 0.83$ (c) and $B_{min}/B_{ECR} = 0.87$ (d).

not measured since the relative intensity of the microwave radiation in the probed frequency range would be obscured by the unknown coupling efficiency between the ion source plasma (source of emission) and the mechanical structure of the ion source (broadcasting "antenna") including non-conductive parts, e.g., high voltage breaks, emitting the radiation to free space. Nevertheless, the described technique allowed detecting the radiation in the whole frequency range of the high-bandwidth oscilloscope (0–25 GHz). Figure 5 shows an example of a typical full-bandwidth spectrogram of the plasma microwave emission during the instability at the following source settings: 4.7×10^{-7} mbar oxygen

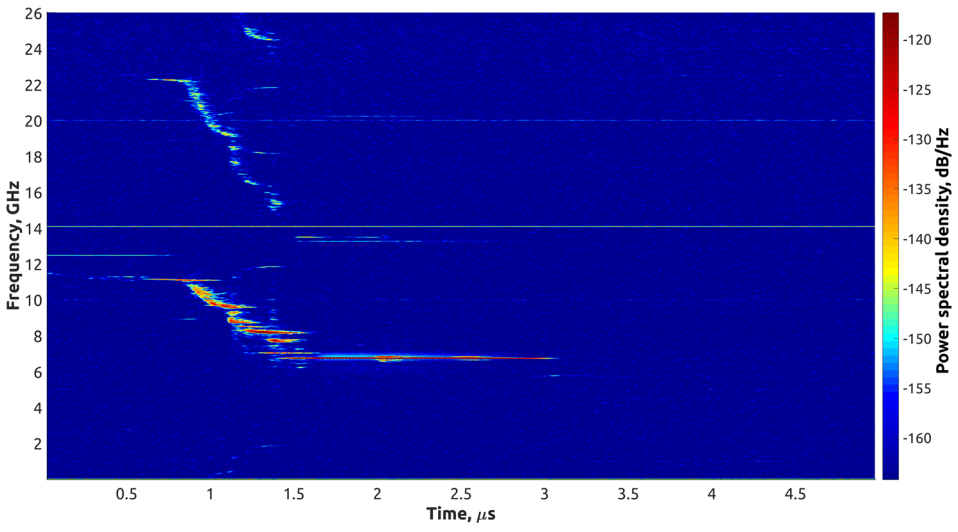

FIG. 5. Spectrogram of an open space microwave emission signal, 4.7×10^{-7} mbar oxygen pressure, 400 W microwave power, B_{min}/B_{ECR} ratio of 0.83.

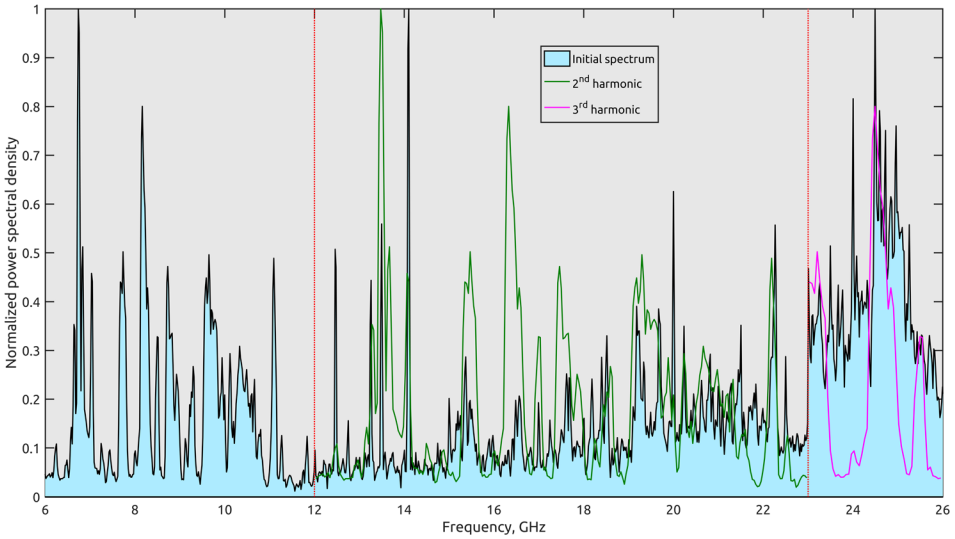

FIG. 6. Fourier spectrum of the open space microwave emission signal, 4.7×10^{-7} mbar oxygen pressure, 400 W microwave power, B_{min}/B_{ECR} ratio of 0.83.

pressure, 400 W microwave power, and B_{min}/B_{ECR} ratio of 0.83. Certain frequencies below 8 GHz are clearly observed.

As it was already pointed out, an important feature which is seen in all spectrograms is that there are at least two groups of frequencies (three in Fig. 5), which seem to correspond to the harmonics of the same process (primary frequency range of 6–12 GHz). To further illustrate this feature, a 2D spectrum of the signal in Fig. 5 is plotted in Fig. 6. The spectrum (filled area) is divided into three regions of interest separated by vertical dotted lines: 6–12 GHz, 12–23 GHz, and 23–26 GHz. In each region, the spectrum is normalized. Finally, the frequencies of the first region are multiplied by a factor of 2 (green curve) and 3 (orange curve), simulating 2nd and 3rd harmonics. These spectra illustrate that the observed emission pattern seems to be formed by the main signal at 6–12 GHz and its second and third harmonics, i.e., $\omega = \frac{n \cdot \omega_{ce}}{\gamma} + k_{\|} \cdot V_{\|}$, where ω is the electron cyclotron frequency, γ is the Lorentz factor, $k_{\|}$ is the longitudinal wavenumber, $V_{\|}$ is the longitudinal electron velocity, and n is the harmonic number ($n = 1, 2, 3$ in the present experiment). In principle, it is possible that all harmonics up to n = 4 are emitted by the plasma of the JYFL 14 GHz ECRIS, as for n = 5 the magnetic field intensity ($B_{max} = 2.05$ T at the injection) is insufficient for the resonant amplification of the microwave signal.

Figure 7 shows the 2D spectrum of the "open space" microwave emission signal combining data from 5000 instability bursts recorded at constant ion source settings.

Similar to previous experiments,[22] dominant frequencies are observed, in particular 12.54, 11.09, and 9.66 GHz. Besides those, there are additional pronounced frequencies (i.e., 6.211, 6.738, 7.051, 8.164, and 25.08 GHz) which can only be observed due to the improved experimental setup.

DISCUSSION

Although the comparison of absolute values of microwave emission intensities is impossible due to the unknown transport function of the microwave detection hardware, the emission frequencies can be measured. A prevailing feature common to all recorded data sets is the falling tone within each instability event. It can therefore be concluded that during the nonlinear amplification of the EM-wave, the energy of the interacting electrons grows with time, as the resonance

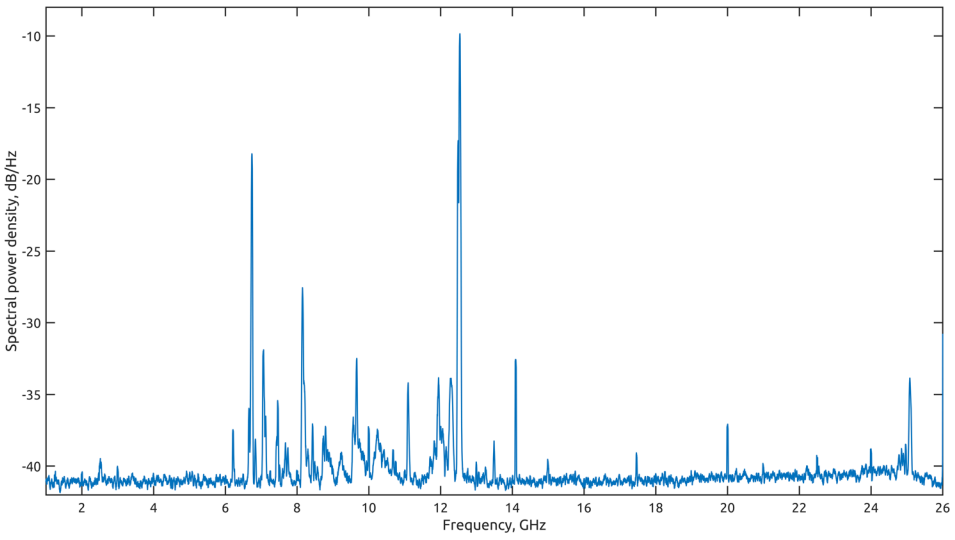

FIG. 7. The spectral power density of the microwave emission signal combining data from 5000 instability bursts. Oxygen pressure 4.7×10^{-7} mbar, microwave power 400 W, B_{min}/B_{ECR} ratio = 0.83.

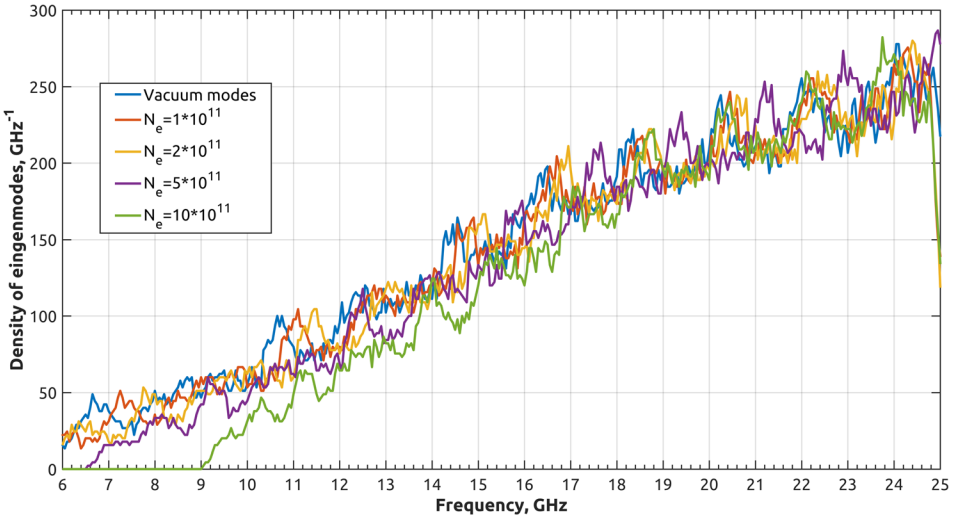

FIG. 8. Simulated density of eigenmode density (modes per 1 GHz) for empty and plasma-loaded cavity.

frequency depends on the electron energy E as $f_R = \frac{28 \cdot B}{1+\frac{E}{511}}$, where f_R is the resonance frequency in GHz, B is the magnetic field in T, and E is the electron energy in keV. This could indicate the presence of a bump in the electron energy distribution function (EEDF), with the instability arising from the low-energy part of the electron population within the bump. In the given energy range, the derivative of the EEDF is positive. The positive slope of the EEDF is then assumed to shift towards higher energies as the developing instability "consumes" electrons, as described in Refs. 25 and 26.

Since the primary emission is observed in the frequency range of 6–12 Ghz, it is possible to estimate the characteristic energy of a bump of the EEDF, which interacts resonantly with the excited electromagnetic wave. The lowest detected emission frequency is 6.211 GHz as shown in Fig. 6. The lowest magnetic field value in the trap for the given spectrum is 0.416 T, which corresponds to a resonance frequency of 11.648 GHz for cold electrons. Hence, in order to interact resonantly with the wave at the lowest observed frequency, the electrons must have an energy of approximately 450 keV (see the equation above). (The estimation does not take into account the Doppler shift, which may reduce the energy.) Such energetic electrons, up to 1 MeV, are often present in ECRIS plasmas as described, e.g., in Ref. 10 and indirectly observed due to thick target bremsstrahlung as described, e.g., in Ref. 27. Based on the results presented here, these energetic electrons accounting for the tail of the EEDF are believed to contribute to the instability and subsequently to the ECRIS performance.

Yet another pronounced feature of the microwave emission is that the dominating frequencies do not depend on the ion source settings. It has been suggested that the interaction of electromagnetic waves and plasma electrons could be strongly affected by the electromagnetic field pattern of the plasma chamber.[28] The existence of such cavity modes could presumably dominate the microwave emission pattern related to kinetic instabilities. This hypothesis was probed experimentally by inserting a 20 mm diameter copper plunger into the plasma chamber (off-axis) through the injection iron plug and varying its penetration depth from 0 (aligned with the injection plug) to 60 mm while observing the emission. It was concluded that changing the cavity dimensions which affects the electromagnetic field pattern of an empty cavity, as explained in Ref. 29, does not affect the dominating microwave emission frequencies which suggests that cavity properties play an insignificant role in determining the interaction between hot electrons and the instability-induced EM-wave. This conclusion is supported further by the simulated spectral density of TE and TM cavity modes shown in Figure 8.

The simulation was performed for empty and uniformly plasma-loaded cylindrical cavity with plasma densities in the range of $1–10 \times 10^{11}\,\mathrm{cm}^{-3}$.

The cavity modes fill the observed frequency range almost uniformly not showing either gaps and/or concentrations in any given frequency ranges, thus supporting the hypothesis that the dominant emission frequencies, which do exhibit such features, may not be defined by cavity modes only, but rather by peculiarities of electron distribution function and the interaction of electrons with plasma waves. At the moment, it is not possible to insist that cavity modes do not play a role, but it is rather obvious that at least one more parameter is responsible for the observed spectral structure of plasma microwave emission.

Although the probable plasma wave mode, i.e., slow extraordinary quasi-longitudinal Z-mode, had been deduced earlier,[22] there are a lot of questions that still remain open to debate. In particular, energies of electrons escaping the confinement due to interaction with plasma waves should be directly measured to confirm the electron energy estimation (0–450 keV). Finally, the EEDF, being the key to the understanding of instabilities, should be studied experimentally. The future research outlined here may help to understand the nature of cyclotron instabilities in ECRIS plasmas and eventually to suppress them in controlled manner.

ACKNOWLEDGMENTS

Authors thank Keysight Technologies Inc. for their technical support. This work has been supported by the EU 7th framework programme "Integrating Activities-Transnational Access," Project No. 262010 (ENSAR), the Academy of Finland under the Finnish Centre of Excellence

Programme 2012–2017 (Nuclear and Accelerator Based Physics Research at JYFL) and researcher mobility Grant Nos. 285895 and 285999. The research of V. Skalyga, D. Mansfeld and I. Izotov was carried out within the state assignment of FASO of Russia (No. 0035-2014-0026).

[1]V. Toivanen, O. Tarvainen, J. Komppula, and H. Koivisto, J. Instrum. **8**, T02005 (2013).
[2]G. S. Taki, P. R. Sarma, R. K. Bhandari, A. G. Drentje, T. Nakagawa, and P. K. Ray, in *Proceedings of the APAC07, TUPMA116*, Indore, India (2007).
[3]B. P. Cluggish, L. Zhao, and J.-S. Kim, Nucl. Instrum. Methods Phys. Res., A **631**, 111–120 (2011).
[4]U. Amaldi, R. Bonomi, S. Braccini, M. Crescenti, A. Degiovanni, M. Garlasché, A. Garonna, G. Magrin, C. Mellace, P. Pearce, G. Pittà, P. Puggioni, E. Rosso, S. Verdú Andrés, R. Wegner, M. Weiss, and R. Zennaro, Nucl. Instrum. Methods A **620**, 563–577 (2010).
[5]A. Denker, H. Homeyer, H. Kludge, and J. Opitz-Coutureau, Nucl. Instrum. Methods B **240**, 61–68 (2005).
[6]D. Leitner, C. M. Lyneis, S. R. Abbott, D. Collins, R. D. Dwinell, M. L. Galloway, M. Leitner, and D. S. Todd, Nucl. Instrum. Methods B **235**, 486 (2005).
[7]H. W. Zhao, L. T. Sun, X. Z. Zhang, and X. H. Guo, Rev. Sci. Instrum. **79**, 02A315 (2008).
[8]T. Antaya and S. Gammino, Rev. Sci. Instrum. **65**, 1060 (1994).
[9]O. Tarvainen, T. Ropponen, V. Toivanen, J. Ärje, and H. Koivisto, Plasma Sources Sci. Technol. **18**, 035018 (2009).
[10]C. Barue, M. Lamoreux, P. Briand, A. Girard, and G. Melin, J. Appl. Phys. **76**, 2662 (1994).
[11]G. Douysset, H. Khodja, A. Girard, and J. P. Briand, Phys. Rev. E **61**, 3015 (2000).
[12]S. V. Golubev and A. G. Shalashov, Phys. Rev. Lett. **99**, 205002 (2007).
[13]G. Melin, C. Barue, F. Bourg, P. Briand, J. Debemardi, M. Delaunay, R. Geller, A. Girard, K. S. Golovanivsky, D. Hitz, B. Jacquot, P. Ludwig, J. M. Mathonnet, T. K. Nguyen, L. Pin, M. Pontonnier, J. C. Rocco, and F. Zadworny, in *Proceedings of the 10th International Workshop on ECR Ion Sources*, Knoxville, TN (1991), p. 1 (ORNL CONF-9011136).
[14]O. Tarvainen, I. Izotov, D. Mansfeld, V. Skalyga, S. Golubev, T. Kalvas, H. Koivisto, J. Komppula, R. Kronholm, J. Laulainen, and V. Toivanen, Plasma Sources Sci. Technol. **23**, 025020 (2014).
[15]O. Tarvainen, J. Laulainen, J. Komppula, R. Kronholm, T. Kalvas, H. Koivisto, I. Izotov, D. Mansfeld, and V. Skalyga, Rev. Sci. Instrum. **86**, 023301 (2015).
[16]O. Tarvainen, T. Kalvas, H. Koivisto, J. Komppula, R. Kronholm, J. Laulainen, I. Izotov, D. Mansfeld, V. Skalyga, V. Toivanen, and G. Machicoane, Rev. Sci. Instrum. **87**, 02A703 (2016).
[17]R. C. Vondrasek, R. H. Scott, R. C. Pardo, and D. Edgell, Rev. Sci. Instrum. **73**, 548 (2002).
[18]V. V. Alikaev, V. M. Glagolev, and S. A. Morozov, Plasma Phys. **10**, 753–774 (1968).
[19]W. B. Ard, R. A. Dandl, and R. F. Stetson, Phys. Fluids **9**, 1498 (1966).
[20]R. C. Garner, M. E. Mauel, S. A. Hokin, R. S. Post, and D. L. Smatlak, Phys. Rev. Lett. **59**, 1821 (1987).
[21]R. C. Garner, M. E. Mauel, S. A. Hokin, R. S. Post, and D. L. Smatlak, Phys. Fluids B **2**, 242 (1990).
[22]I. Izotov, O. Tarvainen, D. Mansfeld, V. Skalyga, H. Koivisto, T. Kalvas, J. Komppula, R. Kronholm, and J. Laulainen, Plasma Sources Sci. Technol. **24**, 045017 (2015).
[23]H. Koivisto, P. Heikkinen, V. Hänninen, A. Lassila, H. Leinonen, V. Nieminen, J. Pakarinen, K. Ranttila, J. Ärje, and E. Liukkonen, Nucl. Instrum. Methods B **174**, 379 (2001).
[24]O. Tarvainen, T. Kalvas, H. Koivisto, T. Ropponen, V. Toivanen, J. H. Vainionpää, A. Virtanen, and J. Ärje, in *Proceedings of the HIAT, Venice*, Italy, 8–12 June (2009).
[25]E. G. Harris, J. Nucl. Energy, Part C **2**, 138 (1961).
[26]R. Z. Sagdeev and V. D. Shafranov, Sov. Phys. JETP **12**(1), 130 (1961).
[27]D. Leitner, J. Y. Benitez, C. M. Lyneis, D. S. Todd, T. Ropponen, J. Ropponen, H. Koivisto, and S. Gammino, Rev. Sci. Instrum. **79**, 033302 (2008).
[28]F. Consoli, L. Celona, G. Ciavola, S. Gammino, F. Maimone, S. Barbarino, R. S. Catalano, and D. Mascali, Rev. Sci. Instrum. **79**, 02A308 (2008).
[29]O. Tarvainen, J. Orpana, R. Kronholm, T. Kalvas, J. Laulainen, H. Koivisto, I. Izotov, V. Skalyga, and V. Toivanen, Rev. Sci. Instrum. **87**, 093301 (2016).